

Chapter 14 e^-e^- Collisions

1 General characteristics of e^-e^- collisions

The primary goal of the linear collider program will be to elucidate new physics at the weak scale. The e^-e^- collider brings a number of strengths to this program. Electron-electron collisions are characterized by several unique features:

- *Exactly Specified Initial States and Flexibility.* For precision measurements, complete knowledge of the initial state is a great virtue. This information is provided optimally in e^-e^- collisions. The initial state energy is well-known for both e^+ and e^- beams, despite small radiative tails due to initial state radiation and beamstrahlung. For e^- beams, however, 85% polarization is routinely obtainable now, and 90% appears to be within reach for linear colliders. The three possible polarization combinations allow one to completely specify the spin S_z , weak isospin I_w^3 , and hypercharge Y of the initial state. One may also switch between these combinations with ease and incomparable flexibility.
- *Extreme Cleanliness.* Backgrounds are typically highly suppressed in e^-e^- collisions. The typical annihilation processes of e^+e^- collisions are absent. In addition, processes involving W bosons, often an important background in e^+e^- collisions, may be greatly suppressed by right-polarizing *both* beams.
- *Dictatorship of Leptons.* In e^+e^- collisions, particles are produced ‘democratically’. In contrast, the initial state of e^-e^- collisions has lepton number $L = 2$, electron number $L_e = 2$, and electric charge $Q = -2$.

With respect to the first two properties, the e^-e^- collider takes the linear collider concept to its logical end. The third property precludes many processes available in e^+e^- interactions, but also provides unique opportunities for the study of certain types of new physics, such as supersymmetry. The physics motivations for the e^-e^- collider have been elaborated in a series of workshops over the past six years [1–3]. In the following, we briefly describe a number of possibilities for new physics in which e^-e^- collisions provide information beyond what is possible in other experimental settings. We then review the accelerator and experimental issues relevant for e^-e^- collisions.

2 Physics at e^-e^- colliders

2.1 Møller scattering

The process $e^-e^- \rightarrow e^-e^-$ is, of course, present in the standard model. At e^-e^- colliders, the ability to polarize both beams makes it possible to exploit this process fully.

One may, for example, define two left-right asymmetries

$$\begin{aligned}
 A_{LR}^{(1)} &\equiv \frac{d\sigma_{LL} + d\sigma_{LR} - d\sigma_{RL} - d\sigma_{RR}}{d\sigma_{LL} + d\sigma_{LR} + d\sigma_{RL} + d\sigma_{RR}} \\
 A_{LR}^{(2)} &\equiv \frac{d\sigma_{LL} - d\sigma_{RR}}{d\sigma_{LL} + d\sigma_{RR}}, \tag{14.1}
 \end{aligned}$$

where $d\sigma_{ij}$ is the differential cross section for $e_i^-e_j^- \rightarrow e^-e^-$ scattering. There are four possible beam polarization configurations. The number of events in each of the four configurations, N_{ij} , depends on the two beam polarizations P_1 and P_2 . Given the standard model value for $A_{LR}^{(1)}$, the values of N_{ij} allow one to simultaneously determine P_1 , P_2 , and $A_{LR}^{(2)}$. For polarizations $P_1 \simeq P_2 \simeq 90\%$, integrated luminosity 10 fb^{-1} , and $\sqrt{s} = 500 \text{ GeV}$, the beam polarizations may be determined to $\Delta P/P \approx 1\%$ [4,5]. Such a measurement is comparable to precisions achieved with Compton polarimetry, and has the advantage that it is a direct measurement of beam polarization at the interaction point.

This analysis also yields a determination of $A_{LR}^{(2)}$, as noted above. Any inconsistency with the standard model prediction is then a signal of new physics. For example, one might consider the possibility of electron compositeness, parameterized by the dimension-six operator $\mathcal{L}_{\text{eff}} = \frac{2\pi}{\Lambda^2} \bar{e}_L \gamma^\mu e_L \bar{e}_L \gamma_\mu e_L$. With $\sqrt{s} = 1 \text{ TeV}$ and an 82 fb^{-1} event sample, an e^-e^- collider is sensitive to scales as high as $\Lambda = 150 \text{ TeV}$ [6]. The analogous reach for Bhabha scattering at e^+e^- colliders with equivalent luminosity is roughly $\Lambda = 100 \text{ TeV}$.

2.2 Higgs bosons

The Higgs boson production mechanism $e^+e^- \rightarrow Zh$ in the e^+e^- mode is complemented by production through WW and ZZ fusion in both e^+e^- and e^-e^- colliders. The study of $e^-e^- \rightarrow e^-e^-h^0$ through ZZ fusion has a number of advantages [7,8]. The cross section is large at high energy, since it does not fall off as $1/s$. The usual backgrounds from e^+e^- annihilation are absent. The final electrons typically have transverse momenta of order m_Z . Thus, one can reconstruct the recoil mass and observe the Higgs boson in this distribution, as shown in Fig. 14.1. Invisible decays of the Higgs boson, and branching ratios more generally, can be studied by this technique.

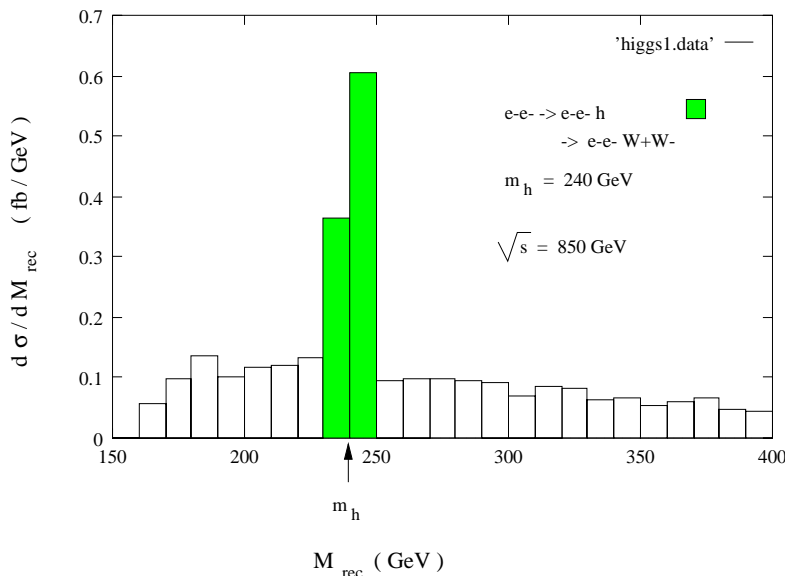


Figure 14.1: Differential cross sections as functions of recoil mass for $e^-e^- \rightarrow e^-e^-h$ and its principal standard model background $e^-e^- \rightarrow e^-e^-W^+W^-$. The Higgs boson mass is $m_h = 240$ GeV, $\sqrt{s} = 850$ GeV, and each electron satisfies an angular cut $\theta_{e^-} > 5^\circ$. From [7].

2.3 Supersymmetry

The e^-e^- mode is an ideal setting for studies of sleptons. All supersymmetric models contain Majorana fermions that couple to electrons—the electroweak gauginos \tilde{B} and \tilde{W} . Slepton pair production is therefore always possible [9], while all potential backgrounds are absent or highly suppressed. Precision measurements of slepton masses, slepton flavor mixings, and slepton couplings in the e^-e^- mode are typically far superior to those possible in the e^+e^- mode. Studies of all of these possibilities are reviewed in Chapter 4, Section 6.1.

The e^-e^- collider may also be used to determine the properties of other superpartners. For example, the production of right-handed selectron pairs is highly sensitive to the Majorana Bino mass M_1 that enters in the t -channel (see Fig. 14.2). As a consequence, extremely high Bino masses M_1 may be measured through the cross section of \tilde{e}_R^- pair production [10]. This region of parameter space is difficult to access in other ways.

2.4 Bileptons

The peculiar initial state quantum numbers of e^-e^- colliders make them uniquely suited for the exploration of a variety of exotic phenomena. Among these are bilep-

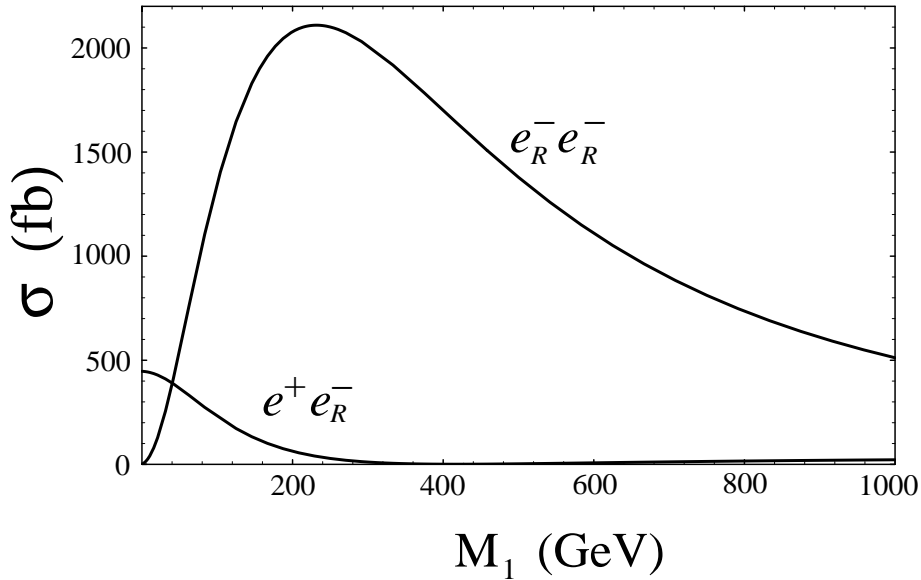


Figure 14.2: The total selectron pair production cross sections for the $e_R^- e_R^-$ and $e^+ e_R^-$ modes with $m_{\tilde{e}_R} = 150$ GeV and $\sqrt{s} = 500$ GeV, as functions of the Bino mass M_1 . From [10].

tons, particles with lepton number $L = \pm 2$. Such particles appear, for example, in models where the $SU(2)_L$ gauge group is extended to $SU(3)$ [11], and the Lagrangian contains the terms

$$\mathcal{L} \supset \left(\ell^- \quad \nu \quad \ell^+ \right)_L^* \begin{pmatrix} & Y^{--} \\ & Y^- \\ Y^{++} & Y^+ \end{pmatrix} \begin{pmatrix} \ell^- \\ \nu \\ \ell^+ \end{pmatrix}_L, \quad (14.2)$$

where Y are new gauge bosons. Y^{--} may then be produced as an s -channel resonance at $e^- e^-$ colliders, mediating background-free events like $e^- e^- \rightarrow Y^{--} \rightarrow \mu^- \mu^-$. Clearly the $e^- e^-$ collider is ideal for such studies.

Bileptons may also appear in models with extended Higgs sectors that contain doubly charged Higgs bosons H^{--} . In these models, both types of particles are produced as resonances in $e^- e^-$ scattering. However, the types of states are clearly distinguished by initial state polarization: bileptons are produced from initial polarization states with $|J_z| = 1$, while doubly charged Higgs particles are produced in channels with $J_z = 0$. The potential of $e^- e^-$ colliders to probe the full spectrum of these models is reviewed in [12].

2.5 Other physics

In addition to these topics, the potential of $e^- e^-$ colliders has also been studied as a probe of strong $W^- W^-$ scattering, anomalous trilinear and quartic gauge boson

couplings, heavy Majorana neutrinos, leptoquarks, heavy Z' bosons, TeV-scale gravity and Kaluza-Klein states, and non-commuting spacetime observables. These topics and other possibilities are discussed in [1–3].

3 Accelerator and experimental issues

3.1 Machine design

There are at present two well-developed approaches to linear collider architecture in the 0.35 to 1 TeV energy range: the NLC/JLC and TESLA designs. Both approaches are easily adaptable to make both e^+e^- and e^-e^- collisions available with relatively little overhead.

The general layout of the NLC design is given in Fig. 14.3. The careful inclusion of the e^-e^- design is described in [13]. The installation of a second polarized electron source presents no difficulty, but magnet polarity reversals and potential spin rotators need to be carefully optimized.

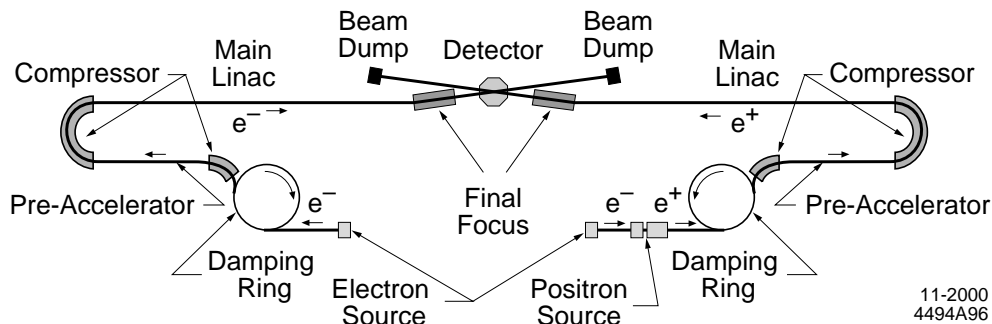


Figure 14.3: Schematic of the NLC. From [13].

Three different modifications for the injection area on the “positron” side have been investigated [14]. We show one of these in Fig. 14.4. In this scheme, the damping ring and bunch compressor for the e^+ beam are used for an e^- beam which circulates in the opposite direction. A new electron gun and some additional components for injection and extraction are needed, but the cost of these is modest, and the switchover from e^+ to e^- operation can be accomplished without significant manual intervention.

For the TESLA project, it is even simpler to introduce polarized e^- through the e^+ injection system. A new polarized electron source is needed, and new components are needed for injection and extraction from the existing positron ‘dogbone’ damping ring [15]. The positions of these new devices mirror the positions of the electron injection and extraction points on the other side of the machine.

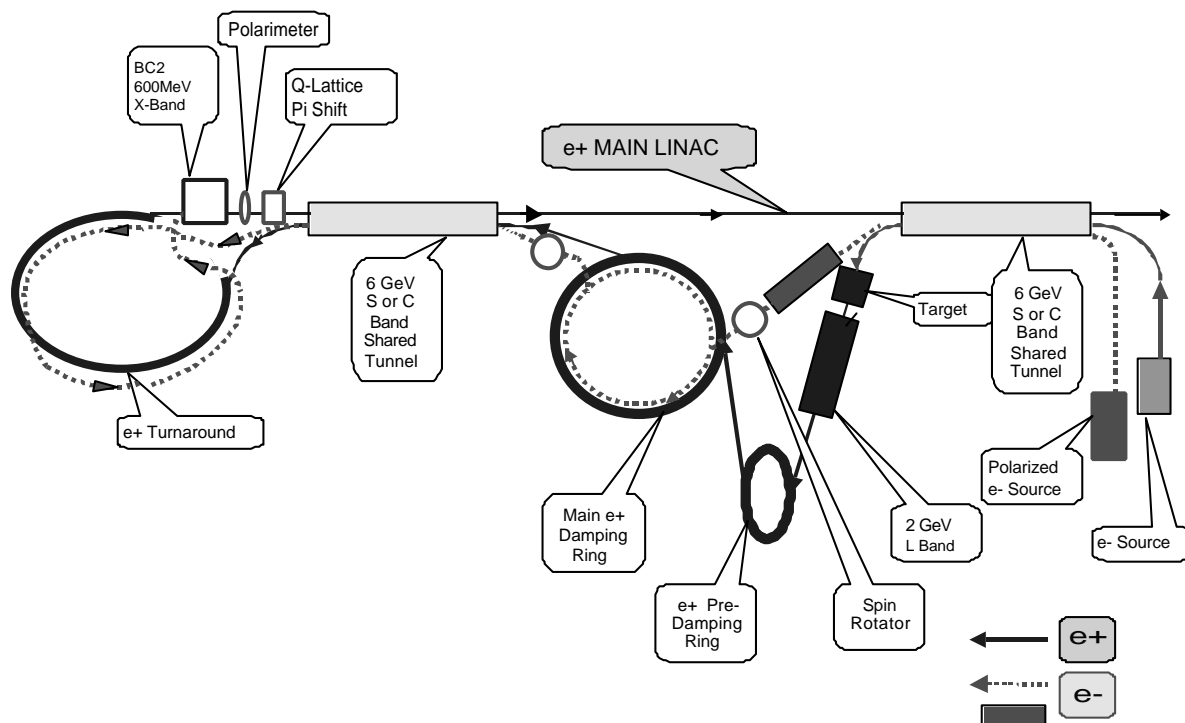


Figure 14.4: The direction reversal model. From [14].

Similar considerations apply to the higher-energy CLIC proposal [16]. As with NLC/JLC and TESLA, the main difficulties involve the injection scheme; once appropriate components are provided, the acceleration of e^- beams and the switchover from e^+e^- to e^-e^- should be straightforward.

3.2 Interaction region

Although e^-e^- operation is straightforwardly incorporated in linear collider designs, experimentation at e^-e^- colliders is not entirely equivalent to that at e^+e^- colliders. This is because the luminosity of the collider is decreased significantly by beam disruption due to the electromagnetic repulsion of the two e^- beams.

Clever manipulation of the beam parameters can minimize the relative luminosity loss; see, for example, [17]. The resulting parameters give about a factor 3 loss for NLC/JLC and a factor 5 loss for TESLA, and do not much reduce the merits of the proposed e^-e^- studies. A plasma lens [18,19] has been proposed to reduce the disruption effects, but this would introduce a serious level of beam-gas backgrounds.

The beamstrahlung effect in e^-e^- is somewhat larger than that in e^+e^- due to the larger disruption, leading to a stronger effective field from the opposite beam. The effect is still modest in size for 500 GeV CM energy. Figure 14.5 shows a comparison of the e^-e^- and e^+e^- cases for the TESLA machine design [20].

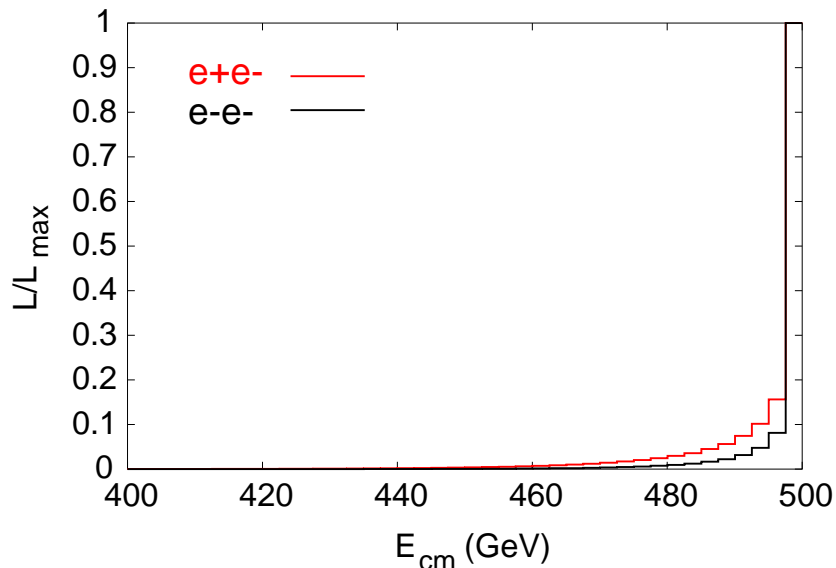


Figure 14.5: Normalized luminosity spectrum for e^-e^- collisions compared to e^+e^- . From [20].

3.3 Detectors

It is important to realize that the detector configuration is easily shared for e^+e^- and e^-e^- experimentation. A caveat exists for beam disposal downstream of the interaction point: if there is any bend upstream of this point, like-sign incoming beams will *not* follow the incoming trajectories of the opposite side, and special beam dumps may have to be configured.

If the linear collider program plans to incorporate $e\gamma$ and $\gamma\gamma$ collisions, with backscattered photon beams, the photon beams must be created from e^- rather than e^+ beams, so that the electron beam polarization can be used to optimize the energy spectrum and polarization of the photon beams. Photon colliders of course have their own, very different, requirements for interaction regions and detectors. These are described in Chapter 13, Section 3.

4 Conclusions

For a number of interesting physics scenarios, the unique properties of e^-e^- colliders will provide additional information through new channels and observables. While the specific scenario realized in nature is yet to be determined, these additional tools may prove extremely valuable in elucidating the physics of the weak scale and beyond. Given the similarities of the e^+e^- and e^-e^- colliders, it should be possible with some

thought in advance to guarantee the compatibility of these two modes of operation and the ease of switching between them. For many possibilities for new physics in the energy region of the linear collider, the small effort to ensure the availability of e^-e^- collisions should reap great benefits.

References

- [1] *Proceedings of the 1st International Workshop on Electron-Electron Interactions at TeV Energies (e^-e^-95)*, Santa Cruz, California, 5–6 September 1995, ed. C. A. Heusch, *Int. J. Mod. Phys.* **A11**, 1523-1697 (1996).
- [2] *Proceedings of the 2nd International Workshop on Electron-Electron Interactions at TeV Energies (e^-e^-97)*, Santa Cruz, California, 22–24 September 1997, ed. C. A. Heusch, *Int. J. Mod. Phys.* **A13**, 2217-2549 (1998).
- [3] *Proceedings of the 3rd International Workshop on Electron-Electron Interactions at TeV Energies (e^-e^-99)*, Santa Cruz, California, 10–12 December 1999, ed. C. A. Heusch, *Int. J. Mod. Phys.* **A15**, 2347-2628 (2000).
- [4] F. Cuypers and P. Gambino, *Phys. Lett.* **B388**, 211 (1996) [hep-ph/9606391].
- [5] A. Czarnecki and W. J. Marciano, *Int. J. Mod. Phys.* **A13**, 2235 (1998) [hep-ph/9801394].
- [6] T. L. Barklow, *Int. J. Mod. Phys.* **A11**, 1579 (1996).
- [7] P. Minkowski, *Int. J. Mod. Phys.* **13**, 2255 (1998).
- [8] J. F. Gunion, T. Han and R. Sobey, *Phys. Lett.* **B429**, 79 (1998) [hep-ph/9801317].
- [9] W. Y. Keung and L. Littenberg, *Phys. Rev.* **D28**, 1067 (1983).
- [10] J. L. Feng, *Int. J. Mod. Phys.* **A13**, 2319 (1998) [hep-ph/9803319].
- [11] P. H. Frampton, *Int. J. Mod. Phys.* **A13**, 2345 (1998) [hep-ph/9711281].
- [12] J. F. Gunion, *Int. J. Mod. Phys.* **A13**, 2277 (1998) [hep-ph/9803222].
- [13] P. Tenenbaum, *Int. J. Mod. Phys.* **A15**, 2461 (2000).
- [14] R. S. Larsen, *Int. J. Mod. Phys.* **A15**, 2477 (2000).
- [15] J. Andruszkow, *et al.*, “TESLA Technical Design Report” (DESY 2001-011/ECFA 2001-209) Vol. II, Chapter 5.
- [16] J. P. Delahaye *et al.*, CERN/PS 98-009 (1998).
- [17] K. A. Thompson, *Int. J. Mod. Phys.* **A15**, 2485 (2000).
- [18] P. Chen, A. Spitkovsky and A. W. Weidemann, *Int. J. Mod. Phys.* **A11**, 1687 (1996).
- [19] J. S. Ng *et al.*, SLAC-PUB-8565, Invited talk presented at the 9th Workshop on Advanced Accelerator Concepts, Santa Fe, New Mexico, 11-16 June 2000.
- [20] I. Reyzl and S. Schreiber, *Int. J. Mod. Phys.* **A15**, 2495 (2000).